DESY 12-166
OUTP-12-19P

Longitudinal momentum shifts, showering and nonperturbative corrections in matched NLO-shower event generators

S. Dooling,[1] P. Gunnellini,[1] F. Hautmann,[2,3] and H. Jung[1,4]

[1] *Deutsches Elektronen Synchrotron, D-22603 Hamburg*
[2] *Theoretical Physics Department, University of Oxford, Oxford OX1 3NP*
[3] *Physics & Astronomy, University of Sussex, Brighton BN1 9QH*
[4] *Elementaire Deeltjes Fysica, Universiteit Antwerpen, B 2020 Antwerpen*

Abstract

Comparisons of experimental data with theoretical predictions for collider processes containing hadronic jets rely on shower Monte Carlo event generators to include corrections to perturbative calculations from hadronization, parton showering, multiple parton collisions. We examine current treatments of these corrections and propose alternative methods to take into account nonperturbative effects and parton showering in the context of next-to-leading-order (NLO) event generators. We point out sizeable parton-showering corrections to jet transverse energy spectra at high rapidity, and discuss kinematic shifts in longitudinal momentum distributions from initial state showering in the case both of jet production and of heavy mass production at the Large Hadron Collider.

I. INTRODUCTION

Phenomenological analyses of collider processes involving the production of hadronic jets rely on event simulation by parton shower Monte Carlo generators [1, 2]. The subject of this paper concerns two different, common uses of shower Monte Carlo generators: one in which they are combined with hard scattering matrix elements via a matching scheme, e.g. at the next-to-leading order (NLO) [3, 4] in perturbative QCD; another in which they are used to obtain corrections to perturbative calculations due to hadronization, showering and multiple parton interactions (see e.g. [5, 6]), with such correction factors then being applied to determine realistic predictions, which can be compared with experimental data.

We begin in Sec. II by considering methods to evaluate the nonperturbative (NP) corrections to jet cross sections using shower event generators. We also estimate the corrections which arise from the initial-state and final-state parton showers and observe that they are sizeable (beyond NLO) in jet transverse energy spectra over the full range of rapidity. We propose a decomposition of the corrections to be applied to fixed NLO calculations, consisting of a truly NP contribution supplemented with a contribution coming from all order resummation via parton showers.

Next, in Sec. III we investigate kinematic aspects of parton showers associated to combining the approximation of collinear, on-shell partons with energy-momentum conservation. The main effect is an event-by-event shift in longitudinal momentum distributions whose size depends on the observable and on the phase space region, and increases with increasing rapidities. We illustrate this by numerical Monte Carlo results in different phase space regions for four specific examples of jet, heavy-quark, electroweak gauge-boson and Higgs boson production. First results on kinematic shifts have been presented in [7].

The approach of this work may be helpful to analyze corrections to finite-order perturbative calculations for jet observables from parton showering and nonperturbative dynamics. These encompass both final-state fragmentation effects and initial-state contributions associated with collinearity approximations. Dynamical high-energy effects on jet final states, distinct from the ones discussed in this paper, have been emphasized in [8–10] due to non-collinear contributions to parton branching processes. We note that both these results and the results in this paper stress the phenomenological relevance of more complete descriptions of QCD parton cascades in terms of transverse momentum dependent parton fragmentation and parton density functions [11–14]. Concluding comments on the results of this work are given in Sec. IV.

II. MONTE CARLO NONPERTURBATIVE CORRECTION FACTORS

In this section we consider methods to evaluate NP and parton shower correction factors. To be definite, we refer to the case of inclusive production of single jets at the LHC [15]. In order to compare theory with experimental data corrected to stable particle level, Refs. [5, 6] supplement NLO perturbative calculations with NP corrections estimated from Monte Carlo event generators. Using leading-order Monte Carlo (LO-MC) generators [1, 2], the correction factors K_0 are schematically obtained by [5, 6]

$$K_0^{NP} = N_{LO-MC}^{(ps+mpi+had)} / N_{LO-MC}^{(ps)} \quad , \tag{1}$$

where $(ps + mpi + had)$ and (ps) mean respectively a simulation including parton showers, multiparton interactions and hadronization, and a simulation including only parton showers

in addition to the LO hard process. Having only LO+PS event generators available, this is the most obvious way to estimate NP corrections to be applied to NLO parton level calculations. However, when these corrections are combined with NLO parton-level results, a potential inconsistency arises because the radiative correction from the first gluon emission is treated at different levels of accuracy in the two parts of the calculation.

We here suggest that an alternative method which avoids this is to use NLO Monte Carlo (NLO-MC) generators to determine the correction. In this case one can consistently assign correction factors to be applied to NLO calculations. Moreover, this method allows one to study separately correction factors to the fixed-order calculation due to parton showering effects. To this end, we introduce the correction factors K^{NP} and K^{PS} as

$$K^{NP} = N^{(ps+mpi+had)}_{NLO-MC}/N^{(ps)}_{NLO-MC} \ , \tag{2}$$

$$K^{PS} = N^{(ps)}_{NLO-MC}/N^{(0)}_{NLO-MC} \ , \tag{3}$$

where the denominator in Eq. (3) is defined by switching off all components beyond NLO in the Monte Carlo simulation. The difference between the correction factors in Eqs. (1) and (2) comes primarily from the way in which the multiple parton interaction (MPI) contribution is matched to the NLO calculation. MPI processes have typical transverse momentum scales smaller than the scale of the hard process, which may be defined as the average transverse momentum of the hard partons. This however is different in LO and NLO calculations, giving rise to non-negligible numerical differences, which we will show below. The correction factor in Eq. (3), on the other hand, is new. It singles out contributions due to parton showering. This correction factor has not been considered in earlier analyses. We show below its numerical significance. We anticipate that taking properly into account these showering corrections can be relevant in fits for parton distribution functions using inclusive jet data.

In Fig. 1 we compute results for the NP correction factors in Eqs. (1),(2) to jet transverse momentum distributions. We define jets using the anti-k$_T$ algorithm [16] with jet size $R = 0.5$ and $R = 0.7$. We plot the results versus the jet transverse momentum p_T for different regions in the jet rapidity y. We show K^{NP} as obtained using the NLO event generator POWHEG [17] and compare it to the result obtained at leading order from PYTHIA [2] (tune Z2 [18] and CTEQ6L1 pdfs [19]). The curves in Fig. 1 illustrate the differences coming from the definition of the hard process.

In Figs. 2 and 3 we compute the corrections from parton shower K^{PS} as obtained from Eq. (3) as a function of the jet p_T for different values of R and different rapidities y. Fig. 2 shows the contributions coming from initial state and final state parton shower separately. In general the effect from parton shower is largest at large $|y|$, where the initial state parton shower is mainly contributing at low p_T, while the final state parton shower is contributing significantly over the whole p_T range.

While the NP corrections studied in Fig. 1 become vanishingly small at sufficiently large p_T, the showering correction in Figs. 2 and 3 gives finite effects also for large p_T . The dependence of this effect on the value of rapidity y will influence the shape of jet distributions and comparisons of theory predictions with experimental data. In particular, if the showering correction factor is not consistently taken into account, besides the NP corrections, this may affect the determination of parton distribution functions from data sets including jets.

Note that in [5, 6] NP correction factors K_0 are applied to the NLO calculation [20], and the data comparison shows that the NLO calculation agrees with data at central rapidities,

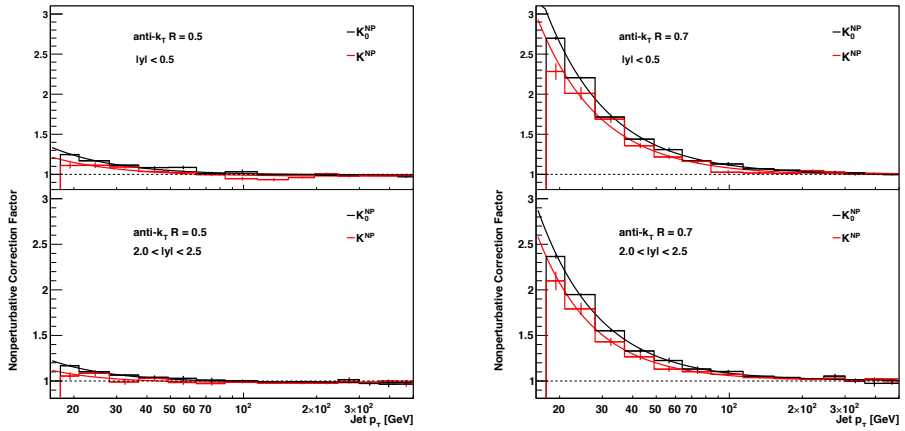

FIG. 1. *The NP correction factors to jet transverse momentum distributions obtained from Eq. (1) and Eq. (2), using* PYTHIA *and* POWHEG *respectively, for* $|y| < 0.5$ *and* $2 < |y| < 2.5$. *Left:* $R = 0.5$*; Right:* $R = 0.7$.

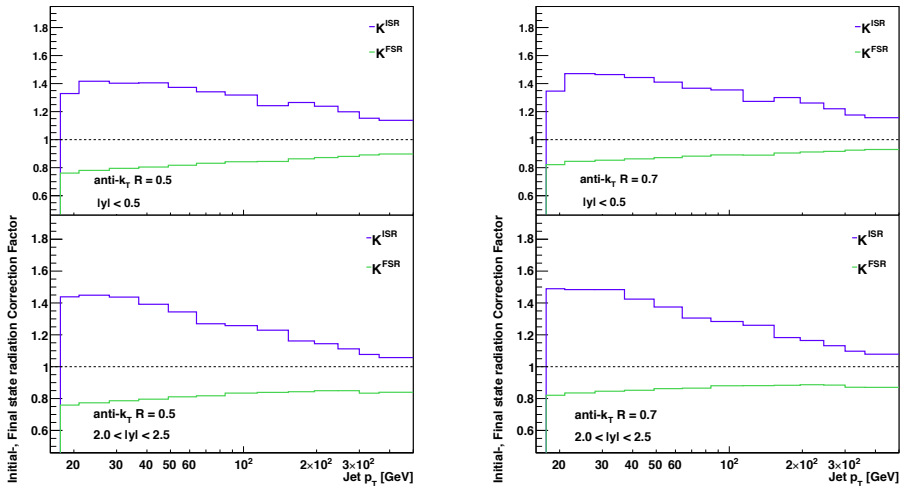

FIG. 2. *The initial and final state parton shower correction factor to jet transverse momentum distributions, obtained from Eq. (3) using* POWHEG *for* $|y| < 0.5$ *and* $2 < |y| < 2.5$. *Left:* $R = 0.5$*; Right:* $R = 0.7$.

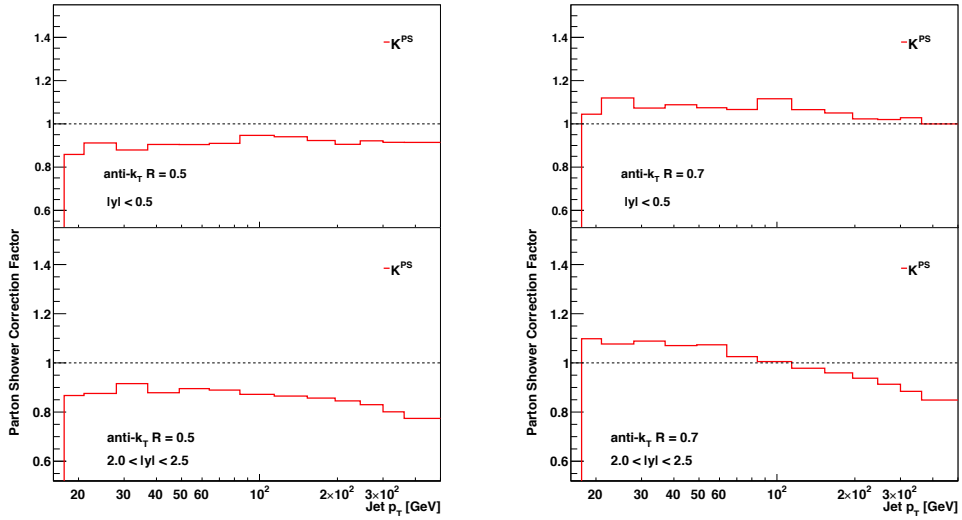

FIG. 3. *The parton shower correction factor to jet transverse momentum distributions, obtained from Eq. (3) using* POWHEG *for* $|y| < 0.5$ *and* $2 < |y| < 2.5$. *Left:* $R = 0.5$*; Right:* $R = 0.7$.

while increasing deviations are seen with increasing rapidity at large transverse momentum p_T [5]. A second comparison is performed in [5] with NLO-matched POWHEG calculations [17], showing large differences in the high rapidity region between results obtained by interfacing POWHEG with different shower models [1, 2] and different model tunes [18, 21]. [1] Motivated by this observation, in the next section we consider more closely the kinematics of the initial state parton shower at high rapidity.

III. INITIAL STATE SHOWERING AND KINEMATIC SHIFTS

Let us recall the physical picture [10] of jet production at high rapidity (Fig. 4) based on QCD high-energy factorization [23]. Take the incoming momenta p_1 and p_2 in Fig. 4 in the plus and minus lightcone directions, and parameterize the exchanged momenta k_1 and k_2 in terms of purely transverse four-vectors $k_{\perp 1}$ and $k_{\perp 2}$ and longitudinal momentum fractions x_i (collinear) and $\overline{x}_i$ (anti-collinear) as $k_1 = x_1 p_1 + k_{\perp 1} + \overline{x}_1 p_2$, $k_2 = x_2 p_2 + k_{\perp 2} + \overline{x}_2 p_1$. To single-logarithmic accuracy in the jet rapidity and the jet transverse momentum, we may approximate k_1 and k_2 using strong ordering in the longitudinal momenta, and get [10]

$$k_1 \simeq x_1 p_1 \quad , \qquad k_2 \simeq x_2 p_2 + k_{\perp 2} \quad , \qquad x_1 \gg x_2 \quad . \tag{4}$$

The physical picture corresponding to the factorization [10, 23] consists of the scattering of a highly off-shell, low-x parton off a nearly on-shell, high-x parton. The calculations [10, 22]

[1] Further discussion of parton showering effects on high-rapidity jets may be found in [22].

embody this picture through the longitudinal and transverse momentum dependences of both perturbative and nonperturbative components of the jet cross section, denoted respectively by $\widehat{\sigma}$ and Φ in Fig. 4. In what follows, however, we will not use the specific content of these calculations, but we will simply use the underlying physical picture as a guidance to examine kinematic effects of collinear approximations.

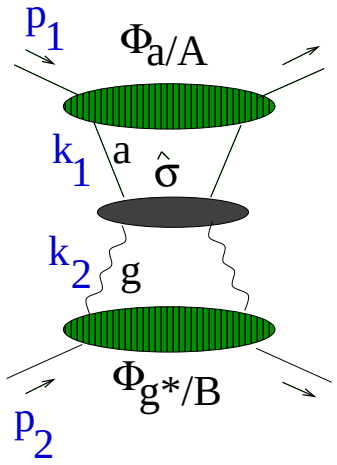

FIG. 4. *Factorized structure of the jet cross section at high rapidity.*

In the light of this picture, let us consider the NLO-matched shower Monte Carlo calculations, following [7]. In the Monte Carlo event generator first the hard subprocess events with full four-momentum assignments for the external lines are generated. In particular, the momenta $k_j^{(0)}$ $(j = 1, 2)$ of the partons initiating the hard scatter are on shell, and are taken to be fully collinear with the incoming state momenta p_j,

$$k_j^{(0)} = x_j p_j \qquad (j = 1, 2) \quad . \tag{5}$$

Next the showering algorithm is applied, and complete final states are generated including additional QCD radiation from the initial-state and final-state parton cascades. As a result of QCD showering, the momenta k_j are no longer exactly collinear,

$$k_j \neq x_j p_j \qquad (j = 1, 2) \quad . \tag{6}$$

Their transverse momentum is to be compensated by a change in the kinematics of the hard scattering subprocess. By energy-momentum conservation, however, this implies a reshuffling, event by event, in the longitudinal momentum fractions x_j of the partons scattering off each other in the hard subprocess. The size of the shift in x_j depends on the emitted transverse momenta.

Let us now focus on jets measured in the rapidity range $y < 2.5$ [6] and examine the effect of the kinematical shift in the longitudinal momentum fractions. To this end we compute the distribution in x_j from POWHEG before parton showering and after parton showering [7]. Fig. 5 shows the distribution for one of the x_j partons. We plot the result before showering (POWHEG) and the results of successively including intrinsic k_t, initial state parton shower and initial+final state parton shower. The results are obtained using the PYTHIA parton shower (tune Z2 [18] and CTEQ6L1 pdfs [19]). This does not include multiple parton interaction and hadronization effects.

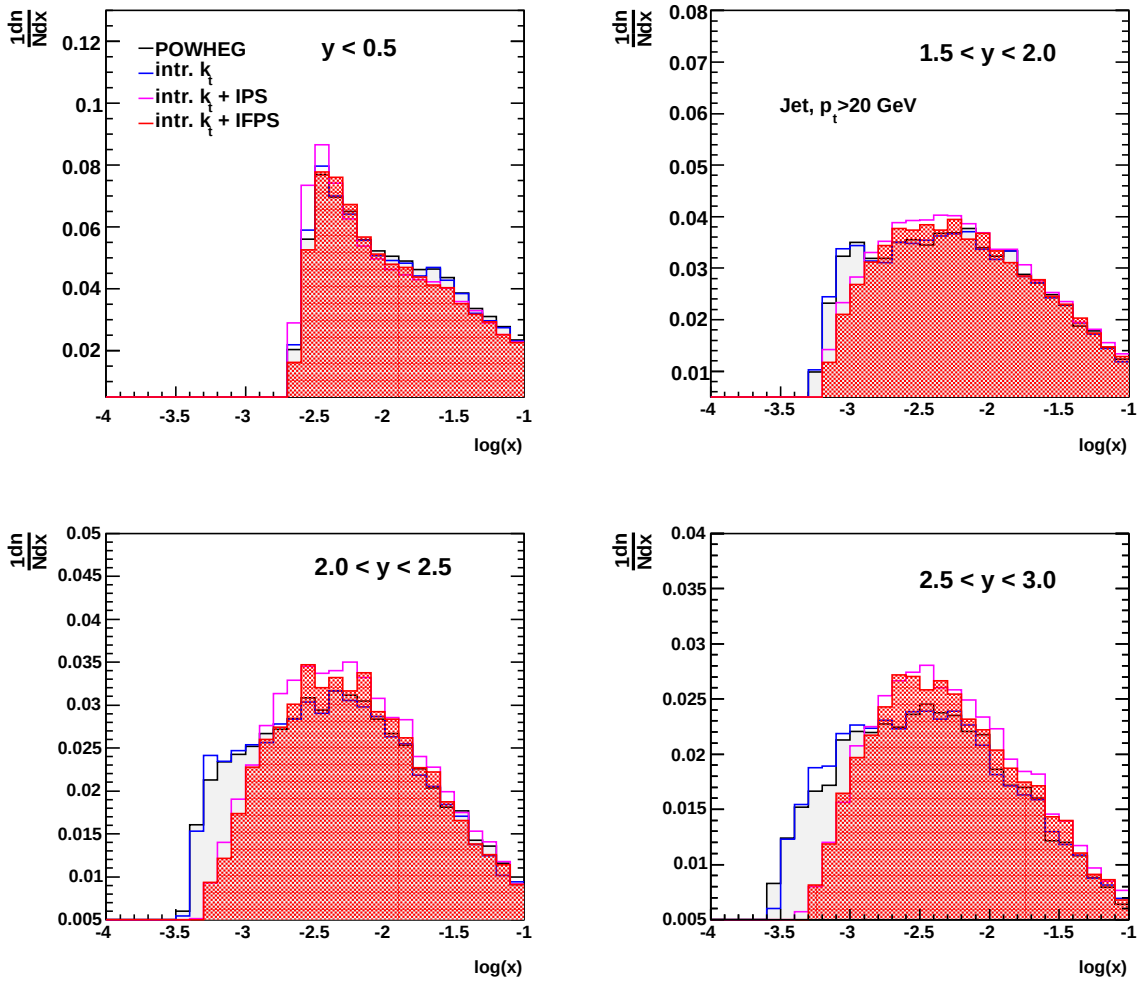

FIG. 5. *Distributions in the parton longitudinal momentum fraction x before (POWHEG) and after parton showering (POWHEG+PS), for inclusive jet production at different rapidities for jets with $p_T > 18$ GeV obtained by the anti-kt jet algorithm [16] with $R = 0.5$. Shown is the effect of intrinsic k_t, initial (IPS) and initial+final state (IFPS) parton shower.*

We see from Fig. 5 that the kinematical reshuffling in the longitudinal momentum fraction is negligible for central rapidities but becomes significant for $y > 1.5$. This effect characterizes the highly asymmetric parton kinematics, which becomes important for the first time at the LHC in significant regions of phase space [10]. Since the perturbative weight for each event is determined by the initial POWHEG simulation, predictions of matched NLO-shower calculations for observables sensitive to this asymmetric region can be affected significantly by the kinematical shift as shown in Fig. 5. Similarly, since the momentum reshuffling is done after the evaluation of the parton distribution functions, the kinematical shift can affect predictions also through the pdfs. It will be of interest to examine the impact of this phase space region on total cross sections as well.

Let us next consider the case of bottom-flavor jet production [24, 25]. The LHC measurements [24, 25] are reasonably described by NLO-matched shower generators MC@NLO [26] and POWHEG [27] at central rapidities, and they are below these predictions at large ra-

pidity and large p_T. In Fig. 6 we consider B-jets in different rapidity regions [24] and plot the gluon x distribution from POWHEG before parton showering and after including various components of the parton shower generator, similarly to what is done above for Fig. 5. We use the PYTHIA parton shower (tune Z2 [18], here including hadronization to identify the B-jet). We observe similar shift in longitudinal momentum with increasing rapidity as in the inclusive jet case.

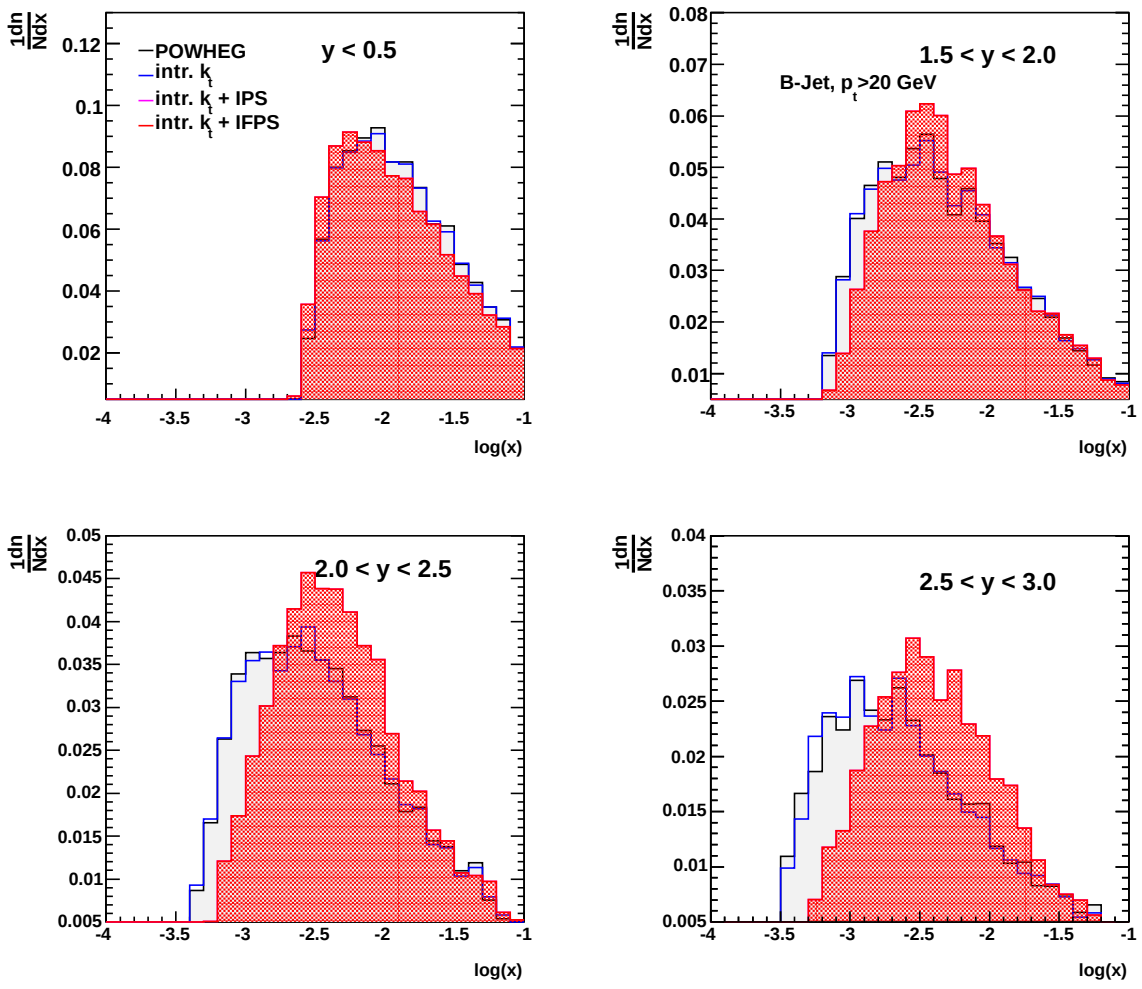

FIG. 6. *Production of b-jets: distribution in the parton longitudinal momentum fraction x, before and after parton showering, for different rapidity regions. Shown is the effect of intrinsic k_t, initial (IPS) and initial+final state (IFPS) parton shower.*

In Fig. 7 we consider Drell-Yan (DY) production in the mass range $16 < m_{DY} < 166$ GeV and perform a similar study to what is done above for jets. In this case too we find that the effects of the kinematical reshuffling in x evaluated from POWHEG become non-negligible away from the central rapidity region. The double peak structure in Fig. 7 comes from the continuum DY production in addition to Z_0 production. It will be of interest to investigate the kinematic reshuffling effect along with the forward Drell-Yan enhancements discussed in [28].

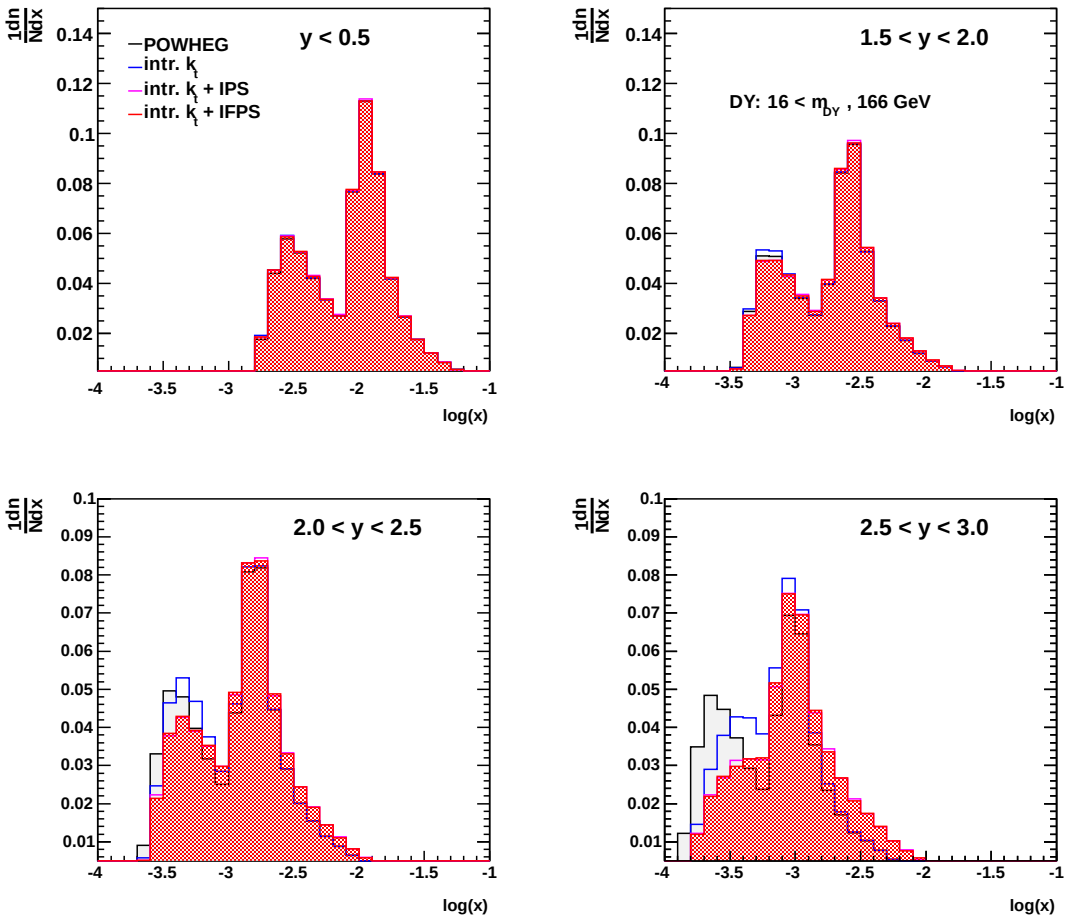

FIG. 7. *Drell-Yan production with* $16 < m_{DY} < 166$ *GeV: distribution in the parton longitudinal momentum fraction* x *before and after showering. Shown is the effect of intrinsic* k_t*, initial (IPS) and initial+final state (IFPS) parton shower.*

Finally we consider Higgs boson production in Fig. 8 for $110 < m_{Higgs} < 130$ GeV. We observe a smaller effect at $\sqrt{s} = 7$ GeV than in the previous cases since the x-range is limited by the Higgs mass.

Fig. 9 summarizes the results in Figs. 5-8 for the ratio of the cross section obtained by POWHEG after inclusion of parton showering to the cross section before parton showering, plotted for different processes. In Fig. 10 we plot this ratio for Higgs boson production at different $\sqrt{s}$ energies of $7, 14$ and 33 GeV.

The longitudinal momentum shifts from parton showering computed in this section measure effects from QCD radiation beyond perturbative fixed-order calculations, and provide a significant contribution to the correction factors in Sec. II. They affect initial-state showers and need to be consistently taken into account in calculations which are used to determine parton density functions. The origin of the kinematical shifts lies with the approximation of collinearity [7] on the partonic states to which the branching algorithms describing showers are applied. Although for explicit calculations we have used a particular NLO-shower matching scheme (POWHEG), the effect is common to any calculation matching NLO with

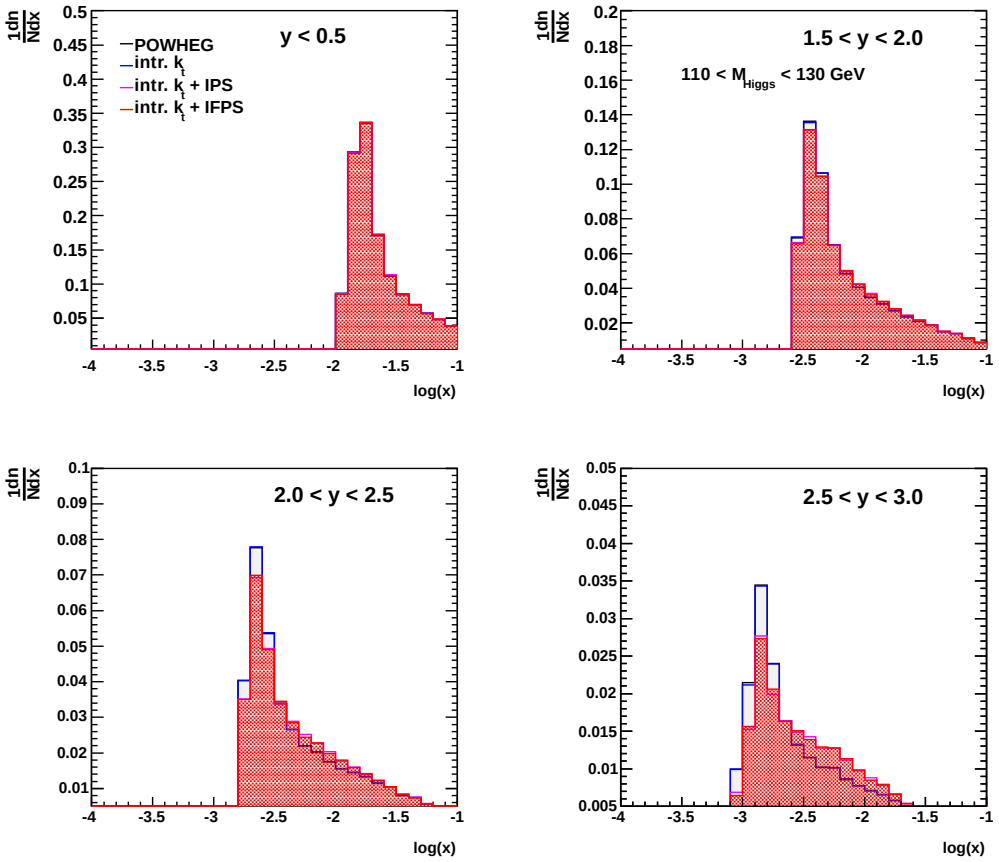

FIG. 8. *Higgs boson production with* $110 < m_{Higgs} < 130$ *GeV: distribution in the parton longitudinal momentum fraction* x *before and after showering. Shown is the effect of intrinsic* k_t*, initial (IPS) and initial+final state (IFPS) parton shower.*

collinear showers. In calculations using integrated parton density functions the correction factors studied in this paper have to be applied after the evaluation of the cross section (and, as remarked on earlier, this may induce systematic inconsistencies if these corrections are not taken into account properly). On the other hand, this is avoided in approaches using transverse momentum dependent PDFs [11–14, 28] from the beginning (TMDs or uPDFs), as is done for example in the CASCADE event generator [29].

IV. CONCLUSIONS

Theoretical predictions for high-energy collider processes containing hadronic jets require supplementing finite-order perturbative calculations with parton showering and nonperturbative corrections. In this paper we have studied methods to treat parton showering and nonperturbative corrections in the context of matched NLO-shower event generators.

We have pointed out potential inconsistencies in current approaches which on the one hand apply NP correction factors from leading-order Monte Carlo generators to NLO parton-level predictions and on the other hand fail to include showering corrections. We have proposed methods to address these deficiencies by using consistently available NLO Monte

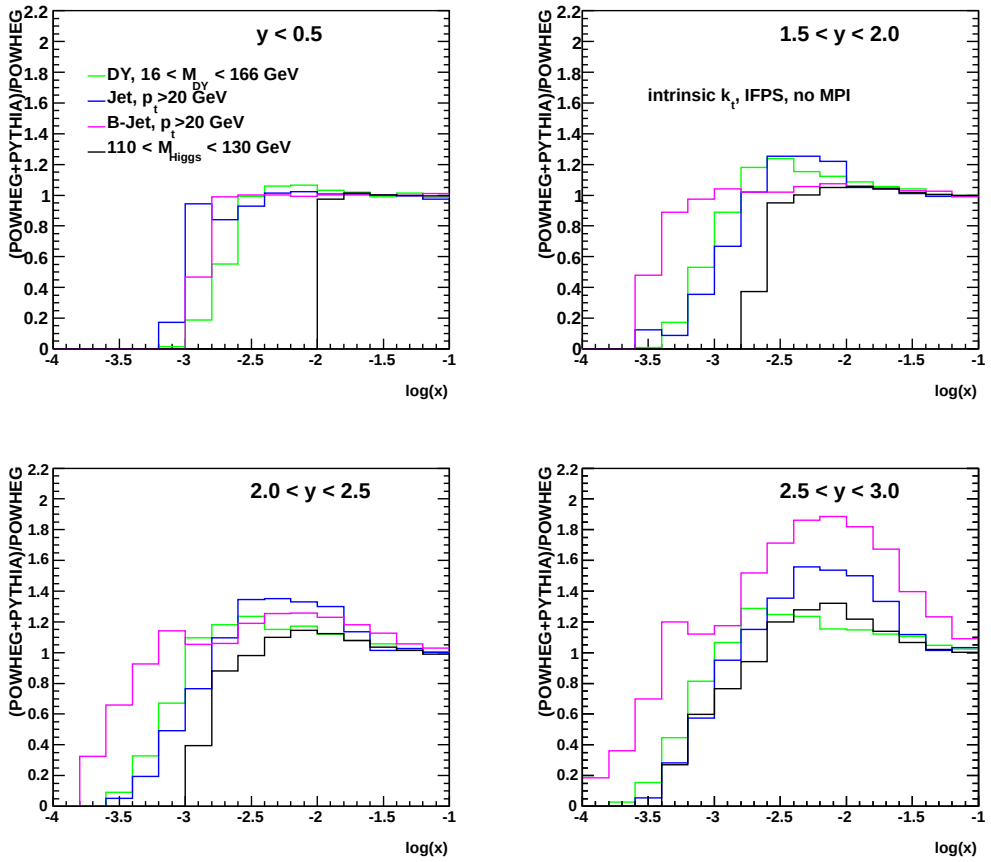

FIG. 9. *Ratio of the cross sections obtained with* POWHEG *after and before inclusion of initial + final state parton shower and intrinsic k_t for the different processes.*

Carlo tools. We have shown that the differences in the predictions for jet cross sections induced by the modified approach we propose are significant in regions of phase space which are explored with hard probes for the first time at the LHC. In particular, the nonperturbative correction factor K^{NP} introduced in Sec. II gives non-negligible differences at low to intermediate jet p_T, and the showering correction factor K^{PS} of Sec. II gives significant effects over the whole p_T range and is largest at large jet rapidities y.

Because of this y and p_T dependence, taking properly into account NP and showering correction factors changes the shape of jet distributions and affects significantly the comparison of theory predictions with experimental data. The numerical results we have presented show effects as large as 50 percent in regions of y and p_T phase space relevant to jet measurements at the LHC. The showering correction factor K^{PS} in particular can affect the determination of parton distribution functions from fits to experimental data sets comprising inclusive jet measurements.

We have investigated in closer detail the sources of the showering correction from initial-state and final-state effects. We have observed that the main initial-state showering effect comes from kinematical shifts in longitudinal momentum distributions [7] due to combining collinearity approximations with the Monte Carlo implementation of energy-momentum conservation constraints. We have examined the longitudinal shifts for specific processes in

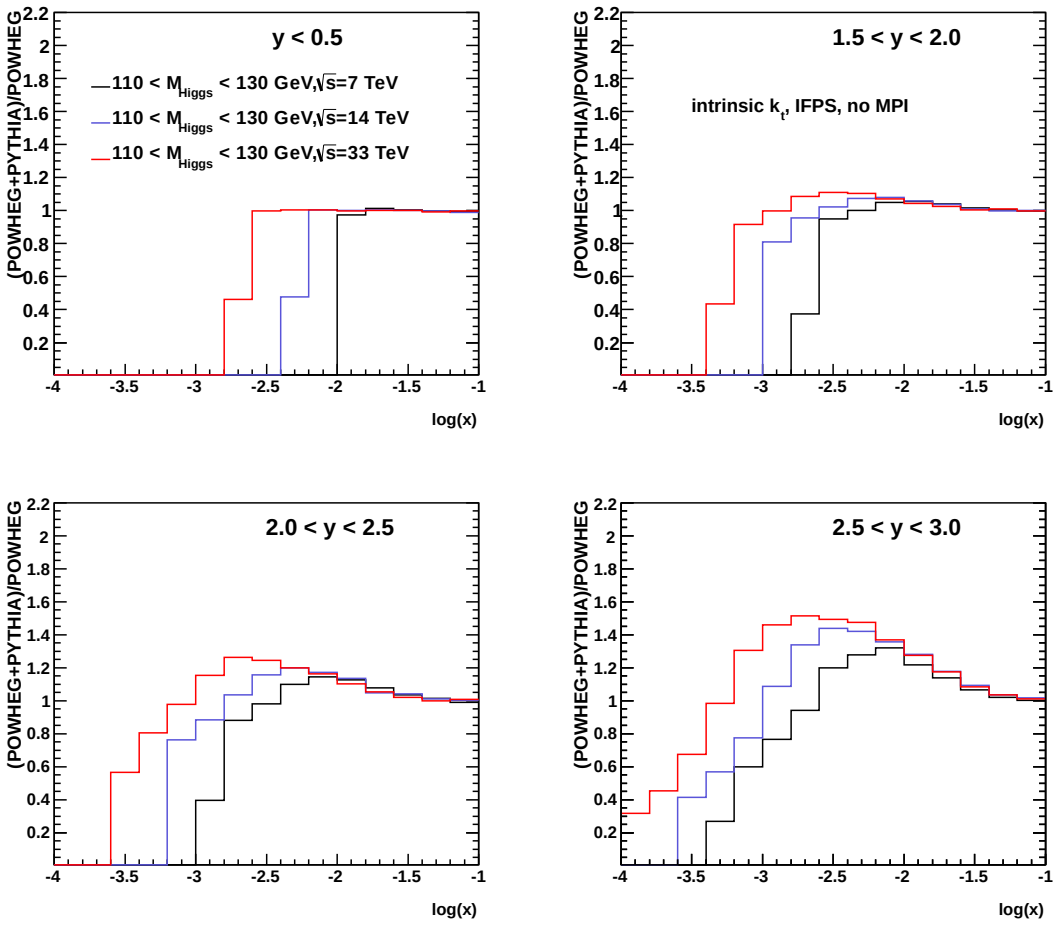

FIG. 10. *Ratio of the cross sections obtained with* POWHEG *after and before inclusion of initial + final state parton shower and intrinsic k_t for Higgs production at different energies:* $\sqrt{s} = 7, 14, 33$ *TeV.*

Sec. III. This effect is largest for inclusive jets and b-flavor jets at the LHC in the higher rapidity bins. We have extended the study of longitudinal shifts [7] to the case of Drell-Yan pair production by analyzing the Drell-Yan mass region $16 < m_{DY} < 166$ GeV and found that the shifts are non-negligible for Drell-Yan production at forward rapidities $y \geq 2$. We have also examined the case of Higgs boson production for $110 < m_{Higgs} < 130$ GeV and found that the shifts are non-negligible at large rapidities at $\sqrt{s} = 7$ GeV, and become more and more important at higher centre-of-mass energies.

It will be interesting to study the impact of the effects discussed in this work on phenomenological analyses of LHC final states involving hadronic jets. We expect these effects to also influence determinations of parton distributions. Longitudinal momentum shifts can be avoided in formulations that keep track of non-collinear (i.e., transverse and/or anti-collinear) momentum components from the beginning using unintegrated initial-state distributions [12, 13], also at parton shower level [29, 30]. It will be interesting to investigate to what extent this can be exploited to construct approaches in which nonperturbative contributions such as multiple parton interactions, finite transverse momenta, hadronization

are consistently incorporated in parton branching event generators.

ACKNOWLEDGEMENTS

We are grateful to Torbjörn Sjöstrand for many discussions concerning hadronisation corrections and multi-parton interactions in PYTHIA. We are also grateful for many discussions and clarifications on POWHEG to Simone Alioli.

---

[1] G. Corcella et al., JHEP **0101** (2001) 010 [arXiv:hep-ph/0011363]; G. Corcella et al., arXiv:hep-ph/0210213.
[2] T. Sjöstrand, S. Mrenna and P. Skands, JHEP **0605** (2006) 026.
[3] P. Nason and B.R. Webber, arXiv:1202.1251 [hep-ph].
[4] S. Höche, SLAC preprint SLAC-PUB-14498 (2011); S. Höche and M. Schönherr, arXiv:1208.2815 [hep-ph].
[5] ATLAS Coll. (G. Aad et al.), Phys. Rev. D **86** (2012) 014022.
[6] S. Chatrchyan *et al.* [CMS Collaboration], Phys. Rev. Lett. **107** (2011) 132001 [arXiv:1106.0208 [hep-ex]].
[7] F. Hautmann and H. Jung, arXiv:1209.6549 [hep-ph].
[8] G. Marchesini and B.R. Webber, Nucl. Phys. **B386** (1992) 215.
[9] F. Hautmann and H. Jung, JHEP **0810** (2008) 113.
[10] M. Deak et al., JHEP **0909** (2009) 121; arXiv:0908.1870; Eur. Phys. J. C **72** (2012) 1982.
[11] J.C. Collins, *Foundations of perturbative QCD*, CUP 2011.
[12] E. Avsar, arXiv:1203.1916 [hep-ph]; arXiv:1108.1181 [hep-ph].
[13] F. Hautmann, Acta Phys. Polon. B **40** (2009) 2139; Phys. Lett. B **655** (2007) 26; F. Hautmann and H. Jung, arXiv:0712.0568 [hep-ph]; arXiv:0808.0873 [hep-ph].
[14] P.J. Mulders, Pramana **72** (2009) 83; P.J. Mulders and T.C. Rogers, arXiv:1102.4569 [hep-ph].
[15] K. Rabbertz, review talk at ISMD 2012, Kielce, September 2012.
[16] M. Cacciari, G. Salam and G. Soyez, JHEP **0804** (2008) 063.
[17] S. Alioli et al., JHEP **1104** (2011) 081.
[18] R.D. Field, arXiv:1010.3558 [hep-ph]
[19] J. Pumplin et al., JHEP **0207** (2002) 012.
[20] Z. Nagy, Phys. Rev. D **68** (2003) 094002.
[21] P.Z. Skands, Phys. Rev. D **82** (2010) 074018.
[22] M. Deak et al., arXiv:1206.7090 [hep-ph]; arXiv:1012.6037 [hep-ph].
[23] S. Catani et al., Phys. Lett. B**242** (1990) 97; Nucl. Phys. B**366** (1991) 135; Phys. Lett. B**307** (1993) 147; Phys. Lett. B**315** (1993) 157; Nucl. Phys. B**427** (1994) 475.
[24] CMS Coll. (S. Chatrchyan et al.), JHEP **1204** (2012) 084.
[25] ATLAS Coll. (G. Aad et al.), Eur. Phys. J. C **71** (2011) 1846.
[26] S. Frixione, P. Nason and B.R. Webber, JHEP **0308** (2003) 007.
[27] S. Frixione, P. Nason and G. Ridolfi, JHEP **0709** (2007) 126.
[28] F. Hautmann, M. Hentschinski and H. Jung, Nucl. Phys. B**865** (2012) 54; arXiv:1205.6358 [hep-ph]; arXiv:1209.6305 [hep-ph].
[29] H. Jung et al., Eur. Phys. J. C **70** (2010) 1237.

[30] S. Jadach and M. Skrzypek, Acta Phys. Polon. B **40** (2009) 2071; S. Jadach, M. Jezabek, A. Kusina, W. Placzek and M. Skrzypek, arXiv:1209.4291 [hep-ph].